NMR Structural Studies of a 15-mer DNA Duplex from a *ras* Protooncogene Modified with the Carcinogen 2-Aminofluorene: Conformational Heterogeneity

Bongsup P. Cho,*,‡,§ Frederick A. Beland,*,‡ and M. Matilde Marques*,∥

Division of Biochemical Toxicology, National Center for Toxicological Research, Jefferson, Arkansas 72079, and Centro de Quimica Estrutural, Complexo I, I.S.T., Av. Rovisco Pais, 1096 Lisboa Codex, Portugal

Received August 19, 1993; Revised Manuscript Received November 5, 1993®

ABSTRACT: Proton NMR studies were conducted on the complementary 15-mer DNA duplex, d(5′-TACTCTTCTT[AF]GACCT)·d(5′-AGGTCAAGAAGAGTA) (designated as the AF-modified duplex). The sequence represents a portion of the mouse c-Ha-*ras* protooncogene and was selectively modified to contain a single *N*-(deoxyguanosin-8-yl)-2-aminofluorene (dG-C8-AF) adduct at the deoxyguanosine corresponding to the first base of codon 61. The AF-modified duplex was found to exist in multiple conformations, with one being predominant (~60%). The exchangeable and nonexchangeable protons belonging to the major conformer were sufficiently well-resolved to allow the assignment of the majority of the base and sugar protons. The one-dimensional proton spectra, as well as the NOE cross-peak patterns associated with this conformer of the AF-modified duplex both in H_2O and D_2O spectra, were strikingly similar to those observed for the major conformer of an analogous duplex containing *N*-(deoxyguanosin-8-yl)-4-aminobiphenyl (dG-C8-ABP) in the same position [Cho, B. P., Beland, F. A., & Marques, M. M. (1992) *Biochemistry 31*, 9587–9602]. The experimental results suggest that the AF- and ABP-modified duplexes adopt essentially identical major conformations, with each arylamine moiety being positioned in the major groove of a slightly disturbed B-type DNA duplex. Nonetheless, the absence of specific NOE cross peaks in the vicinity of the modification site indicates that the local structural perturbation is more severe in the AF-modified duplex. Although insufficient data precluded a detailed characterization of the minor conformers of the AF-modified duplex, the observation of significant shielding of the AF aromatic protons suggests a more dramatic structural alteration at the adduct site, possibly involving extensive stacking with the neighboring bases. The higher content (30–40%) of the minor conformers observed for the AF-modified duplex contrasted with the low contribution (5–10%) of similar structures in the ABP-modified duplex and may be attributed to a better overlapping efficiency of the planar AF ring with the nearby bases. Since the significant local perturbation observed in the minor conformers could provide a possible mechanism for mutations, our results support the view that the structural differences in the arylamine fragments of otherwise identical adducts have a direct influence on the conformational heterogeneities, which in turn may play a significant role in arylamine carcinogenesis.

Arylamines and amides have long been regarded as a major class of environmental carcinogens of epidemiological significance since they induce tumors at various organs in experimental animals and are human bladder carcinogens (Beland & Kadlubar, 1990). Upon metabolic activation, these carcinogens are converted into electrophilic intermediates that can bind to DNA to produce covalent adducts, of which the major and most persistent in vivo are C8-substituted deoxyguanosine derivatives. Since the occurrence of DNA damage may cause heritable changes, the formation of covalent DNA adducts is thought to be a critical step in the multistage tumorigenic process.

A considerable amount of evidence has indicated that the local conformational alterations induced by DNA adduct formation may provide the molecular basis for the differences in the rates of repair and mutational specificities often exhibited by structurally similar adducts (Beland & Kadlubar, 1990). Conformation-oriented analyses have been conducted most extensively using reactive derivatives of the carcinogen, 2-(acetylamino)fluorene (AAF).[1] According to most spectroscopic and theoretical studies (Sage & Leng, 1980; Leng et al., 1980; Evans et al., 1980; Lipkowitz et al., 1982; Broyde & Hingerty, 1983; Hingerty & Broyde, 1986; van Houte et al., 1987, 1988), the presence of *N*-(deoxyguanosin-8-yl)-2-aminofluorene (dG-C8-AF), which is the major persistent adduct found in mammalian tissues upon in vivo administration of AAF or the parent amine, 2-aminofluorene (AF) (Beland & Kadlubar, 1990), does not cause substantial helix perturbation. These studies have suggested that the normal anti conformation is accessible to the modified deoxyguanosine and that the AF moiety will reside preferentially in the major groove of a relatively undisturbed B-type DNA duplex.

The marked difference in the mutagenicities and the target organ specificities in experimental animals exhibited by structurally related arylamines, such as AF and the human bladder carcinogen 4-aminobiphenyl (ABP) (Beland & Kadlubar, 1990), provides evidence that the nature of the aryl

* Correspondence may be addressed to any of the authors.
‡ National Center for Toxicological Research.
§ Current address: Department of Medicinal Chemistry, College of Pharmacy, University of Rhode Island, Kingston, RI 02881.
∥ Centro de Quimica Estrutural.
® Abstract published in *Advance ACS Abstracts,* January 15, 1994.

[1] Abbreviations: AAF, 2-(acetylamino)fluorene; ABP, 4-aminobiphenyl; AF, 2-aminofluorene; A_{260}, absorbance at 260 nm; COSY, correlation spectroscopy; dG-C8-ABP, *N*-(deoxyguanosin-8-yl)-4-aminobiphenyl; dG-C8-AF, *N*-(deoxyguanosin-8-yl)-2-aminofluorene; EDTA, ethylenediaminetetraacetic acid; FID, free induction decay; NMR, nuclear magnetic resonance; NOE, nuclear Overhauser effect; 1D, one-dimensional; TSP, 3-(trimethylsilyl)propionate-*2,2,3,3-d*$_4$; 2D, two-dimensional; NOESY, two-dimensional nuclear Overhauser effect spectroscopy.

0006-2960/94/0433-1373$04.50/0

moiety has a major impact on the biological activity of arylamine carcinogens. Early NMR and theoretical work on *N*-(deoxyguanosin-8-yl)-4-aminobiphenyl (dG-C8-ABP), the major adduct formed by ABP, has suggested that, similar to dG-C8-AF, the ABP adduct may be accommodated in the major groove of a slightly distorted DNA duplex (Kadlubar et al., 1982; Shapiro et al., 1986; Lasko et al., 1987). However, the lack of planarity of the two phenyl rings in ABP appears to be responsible for a lower stacking efficiency of dG-C8-ABP with the nearby bases, as compared to dG-C8-AF (Shapiro et al., 1986). This subtle conformational difference between the two adducts may explain the lower frameshift mutagenicity of dG-C8-ABP in *Salmonella typhimurium* TA1538, its relative resistance to DNA repair enzymes in the livers of dogs (Beland & Kadlubar, 1990), and its lower efficiency in inducing hepatic tumors in mice (Beland et al., 1992).

The task of understanding how structurally similar arylamine–DNA adducts can lead to different mutagenicities and repair rates will require three-dimensional structural details of the modification sites. Although NMR methods have been used extensively for this purpose (Evans et al., 1980, 1984; Evans & Miller, 1982; Evans & Levine, 1987, 1988; Sharma & Box, 1985; Shapiro et al., 1986), the number of reported solution NMR studies of intact arylamine–DNA adducts at the duplex level is small (Norman et al., 1989; Cho et al., 1992; O'Handley et al., 1993). This is due in part to the spectral complexities encountered in the proton NMR spectra of modified duplex oligomers (Harris et al., 1988) and to the technical difficulties in preparing carcinogen-modified oligonucleotides (Basu & Essigmann, 1988).

We have recently reported (Cho et al., 1992) the proton NMR study of a complementary 15-mer duplex, d(5'-TACTCTTCTT[ABP]GACCT)·d(5'-AGGTCAAGAAGAG-TA), containing a single dG-C8-ABP adduct located at the first base of codon 61 in a portion of the mouse c-Ha-*ras* protooncogene (designated as the ABP-modified duplex). The modified base is the site of a G→T transversion in hepatomas from male B6C3F1 mice treated with AAF derivatives (Wiseman et al., 1986). The results of our study indicated that the ABP-modified duplex exists in solution as an equilibrium mixture of at least two slowly exchanging conformations, with one being major (>90%). Although a small perturbation was noted in the vicinity of the adduct site, the NOE pattern found for the major conformer indicated that the ABP fragment should reside in the major groove of a weakly distorted B-type DNA duplex. This structure was consistent with earlier predictions based on spectroscopic and theoretical studies (Broyde et al., 1985; Shapiro et al., 1986). On the other hand, the minor conformation, which we estimated to account for 5–10% of the total, appeared to have extensive stacking of the ABP moiety with the neighboring bases.

In the present article, we report a similar NMR study of the same 15-mer DNA duplex, selectively modified to contain dG-C8-AF instead of dG-C8-ABP at the single deoxyguanosine of the noncoding strand (designated as the AF-modified duplex). We have observed much higher conformational heterogeneity for this duplex than that previously found for its ABP-modified analogue (Cho et al., 1992). Despite this spectral complication, we have been able to characterize the major conformer of the AF-modified duplex in some detail. To a certain extent, information regarding the structure of minor conformers was also obtained. Possible biological implications of the observed carcinogen-specific conformational heterogeneity will be discussed in terms of the structures of the carcinogens and their mutagenic specificities.

MATERIALS AND METHODS

Sample Preparation. The synthesis and chemical characterization of the coding and noncoding 15-mer strands and selective AF-modification of the noncoding strand have been described (Marques & Beland, 1990). Prior to duplex formation, each 15-mer was dissolved in a buffer consisting of 100 mM NaCl, 10 mM sodium phosphate, and 100 μM disodium EDTA (pH 7.0), loaded on Waters Sep-Pak C18 reversed-phase cartridges [50 absorption units (A_{260})/cartridge], washed with water, and recovered in its sodium form with 40% acetonitrile in water.

Using our previously reported extinction coefficients at 260 nm (Marques & Beland, 1990), the AF-modified duplex was prepared in a 1:1 molar strand ratio by mixing 137 A_{260} of the coding strand, d(5'-AGGTCAAGAAGAGTA), and 116 A_{260} of the AF-modified strand, d(5'-TACTCTTCTT[AF]-GACCT), in 500 μL of a buffer consisting of 100 mM NaCl, 10 mM sodium phosphate, and 100 μM disodium EDTA (pH 7.0). The solution was maintained at 60 °C for 1 h and then at 5 °C for an additional 24 h to ensure complete annealing. For analysis of the nonexchangeable protons, the sample was lyophilized three times from 99.96% D_2O and finally adjusted to 350 μL (~2.5 mM) with 99.996% D_2O (designated as the D_2O buffer). For observation of the exchangeable protons, the samples were dissolved in the same volume of 90% H_2O/10% D_2O (v/v) (designated as the H_2O buffer). The solutions were degassed with argon before capping.

NMR Experiments. All NMR spectra were obtained in the proton configuration on a Bruker AM500 spectrometer operating at 500 MHz. Spectra were recorded in the temperature range 5–67 °C. Probe temperatures were calibrated using deuterated methanol (Van Geet, 1968). Chemical shifts are reported in ppm downfield from internal 3-(trimethylsilyl)propionate-*2,2,3,3-d*$_4$ (TSP).

For observation of the exchangeable protons, one-dimensional (1D) proton spectra in H_2O buffer were collected with 16K data points over a 11 111-Hz sweep width. The H_2O peak was suppressed by using a 1$\underline{3}$3$\underline{1}$ pulse sequence (Hore, 1983), with the carrier frequency set on the H_2O resonance. 1D NOE difference experiments in H_2O buffer were carried out using the same NMR parameters, with resonances being irradiated for 500 ms with the decoupler channel.

For the NOESY spectra in H_2O buffer, the pulse sequence used was {delay–90°–t_1–90°–t_m–1$\underline{3}$3$\underline{1}$–acquire}$_n$, followed by FID collection. The time-proportional phase increment (TPPI) algorithm was used to obtain a phase-sensitive mode (Bodenhausen et al., 1984). The last 90° detection pulse was replaced by a 1$\underline{3}$3$\underline{1}$ pulse to suppress the H_2O signal (Hore, 1983). A total of 512 t_1 spectra was collected and processed by a 2K × 2K 2D Fourier transformation. A total of 320 scans was accumulated in each t_1 dimension. Two dummy scans were used. The sweep width was 11 111 Hz. The recycle delay and mixing time were 1.2 s and 200 ms, respectively. The spectra were phase-cycled with a 20% variation in the mixing time to suppress zero-quantum peaks. The FIDs were subjected to trapezoidal apodization using TM1 = 50 and TM2 = 250 parameters in both dimensions before Fourier transformation. The digital resolution was 10.9 Hz/point in each dimension.

NOESY spectra in D_2O buffer were recorded using the TPPI method, with mixing times of either 100, 150, or 300 ms. A total of 512 t_1 spectra was collected and processed by

Chart 1: Sequential Numbering Scheme of the 15-mer DNA Duplex

5'- T1 A2 C3 T4 C5 T6 T7 C8 T9 T10 @11 A12 C13 C14 T15 -3'

3'- A30 T29 G28 A27 G26 A25 A24 G23 A22 A21 C20 T19 G18 G17 A16 -5'

Chart 2: Structure and Numbering System of *N*-(Deoxyguanosin-8-yl)-2-aminofluorene (dG-C8-AF)

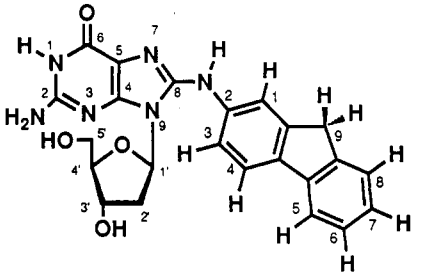

a 2K × 2K 2D Fourier transformation. A total of 240 scans was accumulated in each t_1 dimension, and two dummy scans were used. The sweep width was 4902 Hz. The recycle delay was 1.4 s. The data were apodized with a shifted ($\pi/3$), squared sine-bell apodization function for the t_2 dimension and an unshifted sine-bell apodization function for the t_1 dimension before Fourier transformation. The digital resolution was 4.4 Hz/point in both dimensions. The residual HDO resonance was weakly presaturated.

The COSY experiments in D_2O buffer were acquired in the magnitude mode (Aue et al., 1976). A total of 512 t_1 experiments was collected and processed by a 2K × 1K 2D Fourier transformation. The data were apodized with an unshifted sine-bell window function in both dimensions before Fourier transformation.

RESULTS

The sequential numbering scheme for the AF-modified 15-mer duplex is shown in Chart 1. The sequences labeled from T1 to T15 and from A16 to A30 are the noncoding and coding strands, respectively. The C8-position of the single deoxyguanosine (G11, shadowed) in the noncoding strand was covalently adducted to produce dG-C8-AF, whose structure and numbering system are shown in Chart 2. The structural consequences of the AF modification were probed by comparing the 1D and 2D NMR spectral characteristics of the AF-modified duplex to those of its unmodified and ABP-modified analogues, which we have previously reported (Cho et al., 1992).

Preliminary Analysis of the 1D Proton Spectrum. Figure 1a shows the imino and aromatic proton regions (11.0–14.5 and 6.0–9.0 ppm, respectively) of the 1D proton NMR spectrum of the AF-modified 15-mer duplex recorded in H_2O buffer at 5 °C. At least 16 imino proton resonances of varying intensities were resolved in the downfield region (11.0–14.5 ppm), indicating the existence of more than one conformation in slow equilibrium at 5 °C. A broad and uniquely shielded proton resonance at 11.54 ppm and some low-intensity signals in the range of 13.0–13.5 ppm were additional notable features of this spectrum, since such chemical shifts are not typical for imino protons involved in standard Watson–Crick base pairing (Wüthrich, 1986).

The same regions of the 1D proton spectrum of the analogous ABP-modified 15-mer duplex, recorded under identical conditions (Cho et al., 1992), are plotted for comparison in Figure 1b. The imino proton peaks of the AF-modified duplex (Figure 1a) appeared slightly broader than their counterparts in the ABP-modified duplex (Figure 1b). This suggests that the AF moiety induces a greater extent of conformational heterogeneity, with the broader peaks being due to the partial overlap of close signals from multiple conformers. Nevertheless, with the exception of the uniquely shielded signal at 11.54 ppm (Figure 1a, vide infra), the downfield spectral patterns for the two arylamine-modified duplexes closely resembled one another, which suggested that the duplexes might adopt similar major conformations.

The total contribution of minor conformers to the AF-modified duplex at 5 °C was estimated to be at least 30–40%, which is significantly higher than the 5–10% found for the ABP-modified duplex under the same conditions (Cho et al., 1992). Due to the greater conformational heterogeneity exhibited by the AF-modified duplex, some difficulties were experienced in assigning several exchangeable and nonexchangeable proton signals, particularly those associated with protons located in the vicinity of the modification site. However, some of the uncertainties could be partially overcome by a comparison with the data previously obtained for the ABP-modified duplex. In the following sections, we present a detailed NMR analysis of the major conformer of the AF-

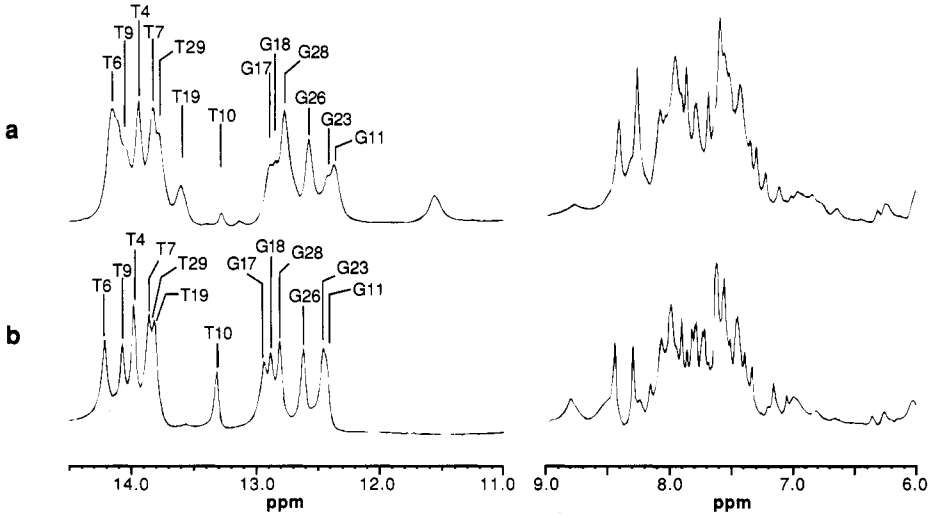

FIGURE 1: 1D 500-MHz proton NMR spectra of (a) the AF-modified 15-mer duplex (this study) and (b) the ABP-modified 15-mer duplex (Cho et al., 1992) in 90% H_2O/10% D_2O containing 100 mM NaCl, 10 mM sodium phosphate, and 100 μM disodium EDTA (pH 7.0) (H_2O buffer) at 5 °C.

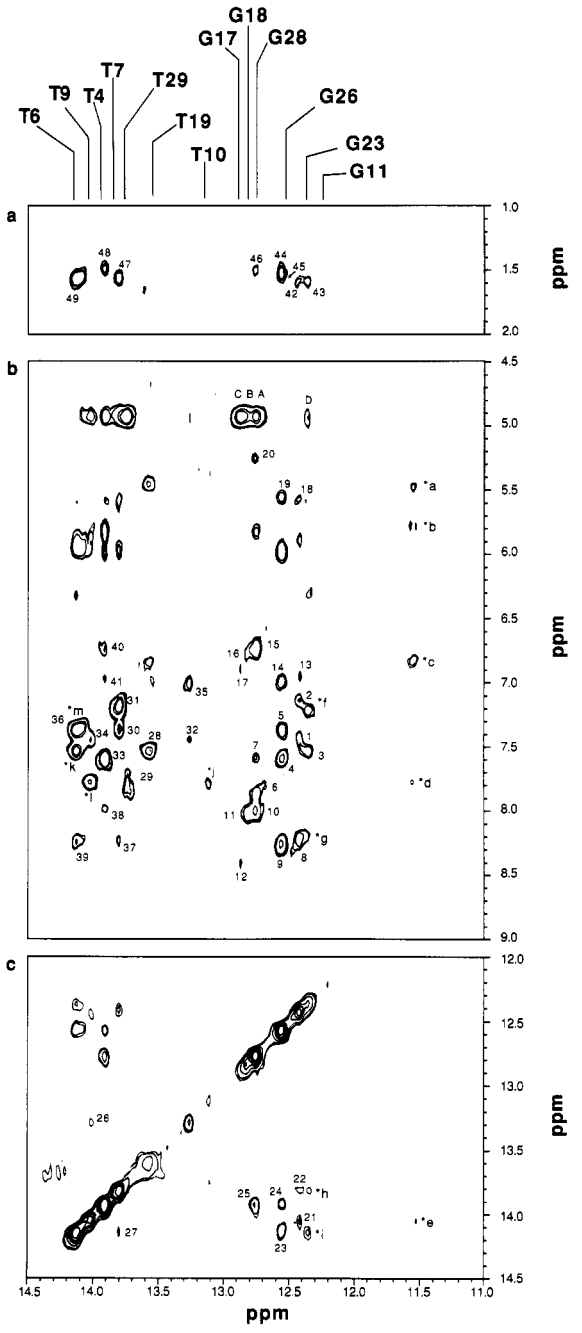

FIGURE 2: Expanded phase-sensitive NOESY contour plots (mixing time 200 ms) of the AF-modified 15-mer duplex, in H_2O buffer at 5 °C. Cross peaks establish connectivities between imino protons (11.0–14.5 ppm) and thymidine methyl protons (1.0–2.0 ppm, region a), base and amino protons (4.5–9.0 ppm, region b), and neighboring imino protons (12.0–14.5 ppm, region c). The labeled cross peaks are assigned as follows: **1**, G23(NH)–A22(H2); **2**, G23(NH)–A24(H2); **3**, G11(NH)–A12(H2); **4**, G26(NH)–A27(H2); **5**, G26(NH)–A25-(H2); **6**, G28(NH)–A2(H2); **7**, G28(NH)–A27(H2); **8**, G23(NH)–C8(NHb); **9**, G26(NH)–C5(NHb); **10**, G28(NH)–C3(NHb); **11**, G18(NH)–C13(NHb); **12**, G17(NH)–C14(NHb); **13**, G23(NH)–C8(NHe); **14**, G26(NH)–C5(NHe); **15**, G28(NH)–C3(NHe); **16**, G18(NH)–C13(NHe); **17**, G17(NH)–C14(NHe); **18**, G23(NH)–C8(H5); **19**, G26(NH)–C5(H5); **20**, G28(NH)–C3(H5); **21**, G23-(NH)–T9(NH); **22**, G23(NH)–T7(NH); **23**, G26(NH)–T6(NH); **24**, G26(NH)–T4(NH); **25**, G28(NH)–T4(NH); **26**, T9(NH)–T10-(NH); **27**, T7(NH)–T6(NH); **28**, T19(NH)–A12(H2); **29**, T29-(NH)–A2(H2); **30**, T7(NH)–A25(H2); **31**, T7(NH)–A24(H2); **32**, T10(NH)–A22(H2); **33**, T4(NH)–A27(H2); **34**, T9(NH)–A22(H2); **35**, T10(NH)–A21(H2); **36**, T6(NH)–A25(H2); **37**, T7(NH)–C8-(NHb); **38**, T4(NH)–C3(NHb); **39**, T6(NH)–C5(NHb); **40**, T4-(NH)–C3(NHe); **41**, T4(NH)–C5(NHe); **42**, G23(NH)–T7(Me); **43**, G11(NH)–T19(Me); **44**, G26(NH)–T6(Me); **45**, G26(NH)–T4(Me); **46**, G28(NH)–T4(Me); **47**, T7(NH)–T7(Me); **48**, T4-(NH)–T4(Me); **49**, T6(NH)–T6(Me); **A**, G28(NH)–H_2O; **B**, G18-(NH)–H_2O; **C**, G17(NH)–H_2O; **D**, G11(NH)–H_2O. Cross peaks marked with asterisked lowercase letters (*a–*m) represent interactions due to minor conformers and were not assigned (see text).

modified duplex and a partial characterization of the minor conformers.

Assignment of the Exchangeable Nucleic Acid Protons

Overall Assignments for the Major Conformer. Three expanded regions of the 200-ms NOESY spectrum of the AF-modified duplex, recorded in H_2O buffer at 5 °C, are shown in Figure 2. The presence of well-shaped cross peaks in this spectrum indicated that the exchange rates of the imino protons were slow under the experimental conditions. The cross peaks in Figure 2 establish the NOE connectivities of each imino proton to its own or neighboring thymidine methyl protons (1.0–2.0 ppm, Figure 2a), to the opposite or adjacent deoxycytidine amino and deoxyadenosine H2 protons (4.5–9.0 ppm, Figure 2b), and to its neighboring imino protons (12.0–14.5 ppm, Figure 2c). The resonance assignments were accomplished through a combined analysis of the 200-ms NOESY (Figure 2) and 1D temperature-dependent proton spectra (Figure 3) (Boelens et al., 1985; Wüthrich, 1986; Wemmer, 1992), as described in our previous study (Cho et al., 1992). Additional confirmation of most of these assignments was achieved by conducting 1D NOE difference experiments (not shown). The chemical shifts for the exchangeable (imino and deoxycytidine amino) protons, as well as the deoxyadenosine H2 protons of the AF-modified duplex, are listed in Table 1, along with the measured differences from their counterparts in the unmodified duplex.

In general terms, the NOE cross-peak patterns associated with the imino protons in the major conformer of the AF-modified duplex were very similar to those observed for its ABP-modified analogue (Cho et al., 1992). These cross peaks were consistent with Watson–Crick base-pair formation throughout the entire length of the AF-modified duplex, with the exception of the frayed oligonucleotide ends (i.e., A16:T15 and A30:T1), for which NOE signals were not detected, and the modification site (i.e., [AF]G11:C20, vide infra). Thus, excluding the AF-modified G11, strong NOE cross peaks were observed between the imino protons of the internal deoxyguanosines (i.e., G18, G23, G26, and G28) and the hydrogen-bonded (peaks 8–11, Figure 2b) and exposed (peaks 13–16, Figure 2b) deoxycytidine amino protons within individual G:C base pairs. Although much weaker, due to fraying effects, the same interactions were also detected for the nearly terminal G17:C14 base pair (peaks 12 and 17, Figure 2b). Furthermore, the range of chemical shift differences (1.26–1.53 ppm, Table 1) between the hydrogen-bonded and exposed amino protons of individual deoxycytidines was comparable to the values found for the corresponding protons in the analogous unmodified and ABP-modified duplexes (Cho et al., 1992) and was also in conformity with the typical differences between the same protons in Watson–Crick G:C base pairs (Boelens et al., 1985). Additionally, the imino protons of the most internal deoxyguanosines (i.e., G23, G26, and G28) displayed strong NOE cross peaks to the nonexchangeable deoxyadenosine H2 protons in adjacent A:T base pairs (peaks 1–2 and 4–7, Figure 2b) and medium to strong NOE cross peaks to the H5 protons of their partner deoxycytidines (peaks 18–20, Figure 2b). These nonexchangeable deoxycytidine (C3, C5, and C8) H5 protons were assigned independently through

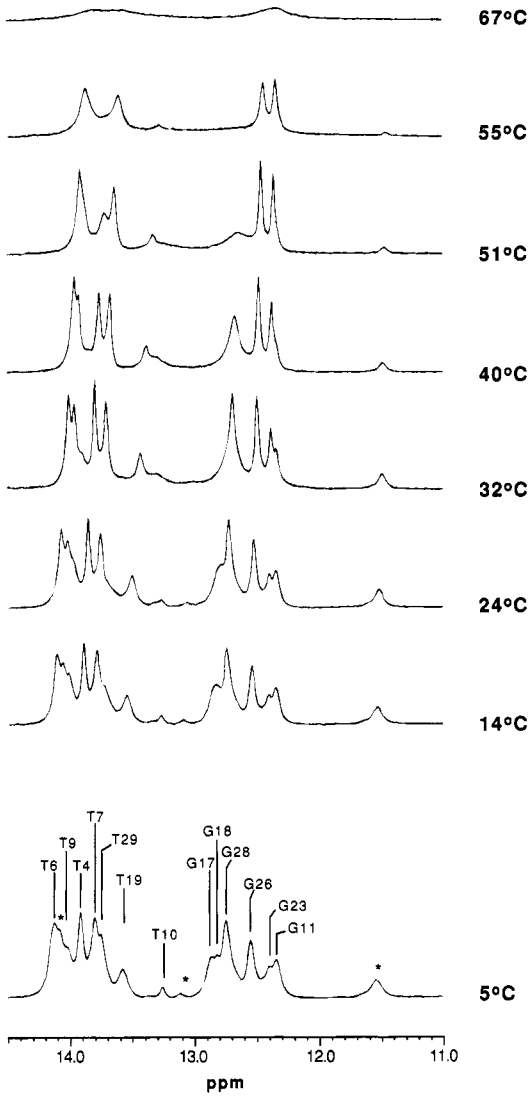

FIGURE 3: Temperature dependence of the imino proton region (11.0–14.5 ppm) of the 1D proton NMR spectra of the AF-modified 15-mer duplex in H_2O buffer. Peaks marked with asterisks are due to the imino protons of minor conformations, which were in slow exchange with the major conformer (see text).

a combined analysis of the NOESY and COSY spectra recorded in D_2O buffer (Figures 4 and 5a, respectively; vide infra).

Fully consistent with the evidence discussed above, strong characteristic NOE cross peaks were observed between the thymidine imino protons belonging to the seven internal A:T base pairs (i.e., A2:T29, A27:T4, A25:T6, A24:T7, A22:T9, A21:T10, and A12:T19) and the deoxyadenosine H2 protons within individual A:T base pairs (peaks 28–29, 31, and 33–36, Figure 2b). Also significant were the NOEs between the imino protons of T7 and T10 and the deoxyadenosine H2 protons of their flanking A25:T6 and A22:T9 base pairs (peaks 30 and 32, respectively, Figure 2b), as well as some weak interactions detected between internal thymidine imino protons and hydrogen-bonded (peaks 37–39, Figure 2b) or exposed (peaks 40–41, Figure 2b) deoxycytidine amino protons in adjacent G:C base pairs.

Exchangeable Protons of the Major Conformer in the Vicinity of the Modification Site. Despite the observation of NOE cross peaks generally consistent with standard Watson–Crick base pairing throughout most of the AF-modified duplex, there was clear evidence of perturbation in the vicinity of the adduct site. Thus, whereas the NOE connectivities between imino protons in flanking base pairs could be traced from G28–T4 to T9–T10 (peaks 21–27, Figure 2c), cross peaks corresponding to the T10–G11, G11–T19, and T19–G18 segments, i.e., involving imino protons located at (G11) or in the vicinity (T10, T19, and G18) of the modification site, could not be detected. Such interruptions, which did not occur in either the unmodified or the ABP-modified 15-mer duplexes (Cho et al., 1992), suggest a significant disturbance in the stacking interactions within a close distance of the AF adduct. Similarly, while a majority of the nonterminal imino proton assignments could be further confirmed through the observation of NOE cross peaks to adjacent (peaks 42–46, Figure 2a) or their own (peaks 47–49, Figure 2a) thymidine methyl protons, the latter interactions were not detected for the base pairs neighboring [AF]G11 (i.e., A22:T9, A21:T10, and A12:T19).

The imino proton of the AF-modified G11 at 12.34 ppm was assigned on the basis of an NOE cross peak to the H2 proton of the adjacent A12 at 7.53 ppm (peak 3, Figure 2b); however, it failed to display an NOE interaction to the H2 proton of A21 at 7.00 ppm. Since this interaction would be expected if the A21:T10–[AF]G11:C20–A12:T19 segment assumed a regular stacked Watson–Crick configuration, its absence presumably reflected a perturbation in the standard interproton distances.

The amino protons of the deoxycytidine opposed to [AF]-G11 (i.e., C20) could not be assigned unambiguously, due to the absence of their mutual NOE interaction in the appropriate region (6.5–9.0 vs 4.5–9.0 ppm, not shown) of the NOESY spectrum. By contrast, all of the mutual NOE connectivities between the H5 and both amino protons of relatively undisturbed deoxycytidines (i.e., C3, C5, and C8, not shown) could be recognized. Inspection of the aromatic region of the 1D proton spectrum (6.0–9.0 ppm, Figure 1a) revealed a very broad peak near 8.8 ppm. A similar resonance in the 1D spectrum of the ABP-modified duplex (Figure 1b) was assigned to the hydrogen-bonded amino proton of C20, which gave a strong NOE cross peak to the imino proton of [ABP]G11 at 12.43 ppm (Cho et al., 1992). Since the major conformers of the AF- and ABP-modified duplexes revealed striking structural similarities, the anticipated NOE interaction between the imino proton of [AF]G11 at 12.34 ppm and the putative hydrogen-bonded amino proton of C20 at 8.8 ppm may have remained undetected as a result of substantial line-broadening. The lack of a definite assignment of the C20 amino protons may be taken as further evidence of significant local structural distortion at the AF modification site. Also consistent with this interpretation was the presence of a moderate exchange cross peak between the imino proton of [AF]G11 and the H_2O resonance at 5.0 ppm (peak D, Figure 2b). Since similar exchange cross peaks were observed for the imino protons of the nearly terminal G17, G18, and G28 (peaks C, B, and A, respectively, Figure 2b), this implies a certain degree of solvent exposure at the modification site.

The T10 imino proton at 13.26 ppm, which was identified on the basis of a weak NOE cross peak to the deoxyadenosine H2 proton of the flanking A22:T9 base pair (peak 32, Figure 2b), was shielded considerably (+0.60 ppm, Table 1) compared to the same imino proton of the parent 15-mer duplex. A similar magnitude of shielding (i.e., +0.54 ppm) was observed for the same proton in the analogous ABP-modified duplex, in which case the perturbation induced by the ABP modification was not sufficient to disrupt the NOE interactions between the imino proton of T10 and the amino protons of C20 (Cho et al., 1992). However, cross peaks consistent with

Table 1: Proton Chemical Shifts for the Major Conformer of the AF-Modified 15-mer Duplex in H_2O Buffer[a] and Chemical Shift Differences from the Corresponding Protons in the Unmodified 15-mer Duplex[b]

	T(NH)/G(NH)		C(NHb)[c]		C(NHe)[d]		A(H2)	
base pair	AF 15-mer	$\Delta\delta$[e]	AF 15-mer	$\Delta\delta$	AF 15-mer	$\Delta\delta$	AF 15-mer	$\Delta\delta$
T1:A30	ND[f]						[g]	
A2:T29	13.73	+0.03					7.85	+0.02
C3:G28	12.76	+0.02	7.99	+0.06	6.73	+0.06		
T4:A27	13.90	+0.05					7.60	–0.02
C5:G26	12.56	+0.02	8.26	+0.03	6.99	+0.08		
T6:A25	14.12	+0.05					7.36	**+0.12**
T7:A24	13.79	+0.05					7.15	–0.03
C8:G23	12.41	+0.04	8.23	+0.06	6.95	+0.08		
T9:A22	14.02	–0.05					7.44	**–0.11**
T10:A21	13.26	**+0.60**					7.00	+0.10
G11:C20	12.34	**+0.18**	NA[h]		NA			
A12:T19	13.56	**+0.15**					7.53	**+0.20**
C13:G18	12.82	0.00	8.03	+0.04	6.76	**–0.14**		
C14:G17	12.87	+0.04	8.41	+0.03	6.88	**+0.11**		
T15:A16	ND						ND	

[a] Chemical shifts are reported in ppm downfield from TSP at 5 °C. Samples were dissolved in 90% H_2O/10% D_2O containing 100 mM NaCl, 10 mM sodium phosphate, and 100 μM disodium EDTA (pH 7.0) (H_2O buffer). [b] Taken from Cho et al. (1992). [c] Hydrogen-bonded deoxycytidine amino proton. [d] Exposed deoxycytidine amino proton. [e] $\Delta\delta$ = δ(unmodified 15-mer) – δ(AF-modified 15-mer); $\Delta\delta > 0.1$ ppm are shown in boldface type. – indicates downfield shift and + indicates upfield shift of protons in the AF-modified 15-mer duplex. [f] ND, not detected. [g] Detected at 7.80 ppm in the NOESY spectrum taken in D_2O buffer (peak f, Figure 4a). [h] NA, not assigned.

such interactions were absent from the NOESY spectrum of the AF-modified duplex.

The temperature-dependent broadening of the imino proton resonances belonging to the major conformer of the AF-modified duplex (Figure 3) was in general agreement with the evidence discussed above. Thus, the imino protons of the nearly terminal G17:C14 and A2:T29 base pairs broadened first, followed by those of G18:C13, A21:T10, A22:T9, and [AF]G11:C20. The imino protons of A12:T19 and A27:T4 were the next to collapse, and subsequent broadening of the remaining internal base pairs then occurred. Although this broadening pattern closely resembled that found for the analogous ABP-modified duplex (Cho et al., 1992), the melting process was slower for the imino proton of [AF]G11 as compared to the same proton of [ABP]G11 in the ABP-modified duplex. This unexpected persistence of the [AF]-G11 imino proton might reflect the presence of an overlapping signal originating from an imino proton of a minor conformer (vide infra). Also significant was the unique deshielding exhibited by the T10 imino proton upon raising the temperature, which may be interpreted as a direct consequence of adduct formation at G11. Identical behavior was observed previously for the same proton in the ABP-modified duplex.

The perturbation detected for the AF-modified duplex in the vicinity of the modification site was reflected by the substantial upfield shifts of the imino protons of [AF]G11 and its neighboring T10 and T19, as compared to the same protons of the unmodified duplex, while the remaining imino protons were virtually unaffected upon incorporation of the AF fragment (Table 1). As previously observed for the ABP-modified duplex (Cho et al., 1992), the magnitude of this shift was more significant for the imino proton of T10, the base flanking the modified G11 in the 5′-direction. This may have been due to a sequence-dependent phenomenon rather than to the nature of the covalent modification. This interpretation is consistent with the facts that A:T base pairs possess intrinsically lower hydrogen-bonding potential than G:C base pairs and that A12:T19 was flanked by two G:C base pairs, whereas A21:T10 was flanked by only one.

Exchangeable Protons of Minor Conformers. The most notable feature of the 1D imino proton spectrum of the AF-modified duplex was the presence of an isolated upfield proton at 11.54 ppm (Figure 1a). This upfield exchangeable proton was not associated with the major conformer of the AF-modified duplex, for which all imino protons were accounted with the exception of the frayed terminal T1 and T15 (vide supra). Additionally, this resonance represented substantial shielding from the typical values found for standard Watson–Crick G:C base pairing (12.0–13.0 ppm). Shieldings of similar magnitude have previously been reported for arylamine-C8-substituted deoxyguanosines in double-stranded oligomers; for example, the imino proton of an AF-modified *syn*-deoxyguanosine opposing an *anti*-deoxyadenosine in an 11-mer DNA duplex occurred at 10.98 ppm (Norman et al., 1989). This imino proton was found to be located in the major groove of the duplex, exposed to H_2O, and not involved in hydrogen-bonding interactions. More recently, the imino proton of an AAF-modified *syn*-deoxyguanosine opposing a deoxycytidine in a 9-mer DNA duplex was found to resonate at 11.88 ppm, with no evidence of hydrogen bonding, and to be protected from the solvent (O'Handley et al., 1993). The same study also provided evidence that the *anti*-deoxycytidine adjacent to the AAF-modified *syn*-deoxyguanosine in the 5′-direction was hydrogen-bonded to an *anti*-deoxyguanosine whose imino proton resonated at 11.45 ppm. Extensive stacking of the AAF moiety with this G:C base pair was invoked to explain the upfield shift exhibited by the imino proton resonance.

With our AF-modified duplex, the signal at 11.54 ppm lacked an exchange NOE cross peak to the H_2O resonance (Figure 2b), but exhibited at least five weak to medium NOE interactions (peaks *a–*d, Figure 2b, and peak *e, Figure 2c) that could not be related to any of the assigned proton resonances of the major conformer (vide supra). This evidence suggested that the imino proton at 11.54 ppm, possibly belonging to the [AF]G11 of a minor conformer, was protected from the solvent and might be hydrogen-bonded. Nevertheless, upon an increase in the sodium ion concentration, the upfield imino proton was gradually shielded and broadened, while the imino protons associated with the major conformer were virtually unchanged (not shown). This observation suggests that the local structure of the minor conformer in the vicinity of the modification site may be sensitive to the ionic strength of the sample preparation.

Several other cross peaks that were not directly related to the major conformer of the AF-modified duplex are marked

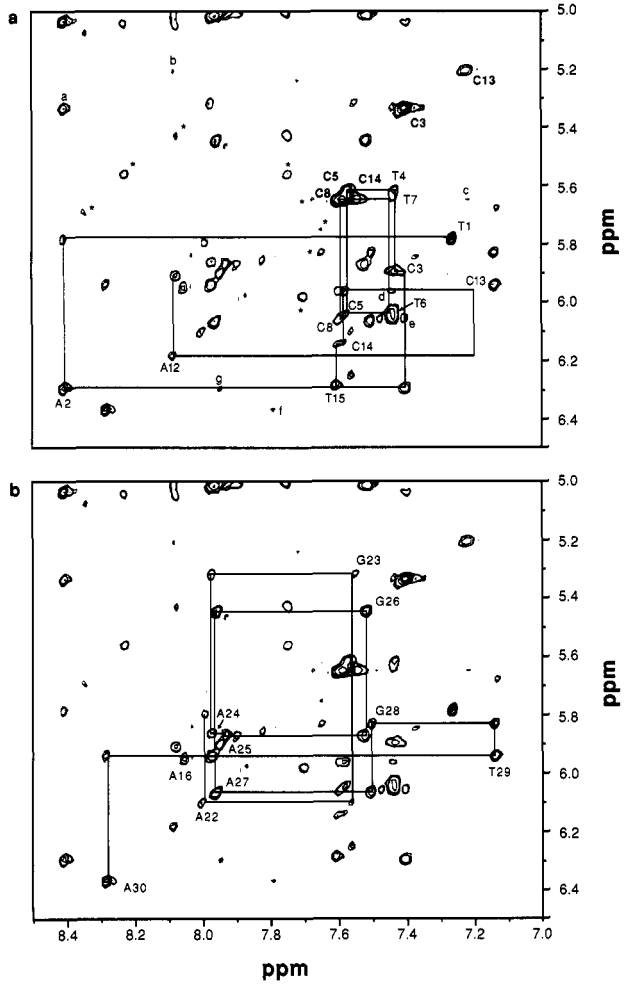

FIGURE 4: Expanded phase-sensitive NOESY contour plots (mixing time 300 ms) of the AF-modified 15-mer duplex, taken at 27 °C in D_2O containing 100 mM NaCl, 10 mM sodium phosphate, and 100 μM disodium EDTA (pH 7.0) (D_2O buffer), establishing connectivities between the base H6/H8 protons (7.0–8.5 ppm) and the sugar H1′ and deoxycytidine H5 protons (5.0–6.5 ppm). The solid lines trace sequential distance connectivities in the noncoding and coding strands (plots a and b, respectively). Cross peaks labeled by base and sequence position are due to intranucleotide sequential NOE connectivities. Cross peaks due to deoxycytidine H5–H6 connectivities are denoted by boldface characters (i.e., **C3**, **C5**, **C8**, **C13**, and **C14**). The remaining cross peaks are assigned as follows: a, A2(H8)–C3-(H5); b, A12(H8)–C13(H5); c, C13(H6)–C14(H5); d, A12(H2)–C13(H1′); e, A22(H2)–C8(H1′); f, A30(H2)–A30(H1′); g, A2(H2)–A2(H1′). Cross peaks marked with asterisks, possibly arising from minor conformers in slow exchange, were not assigned (see text).

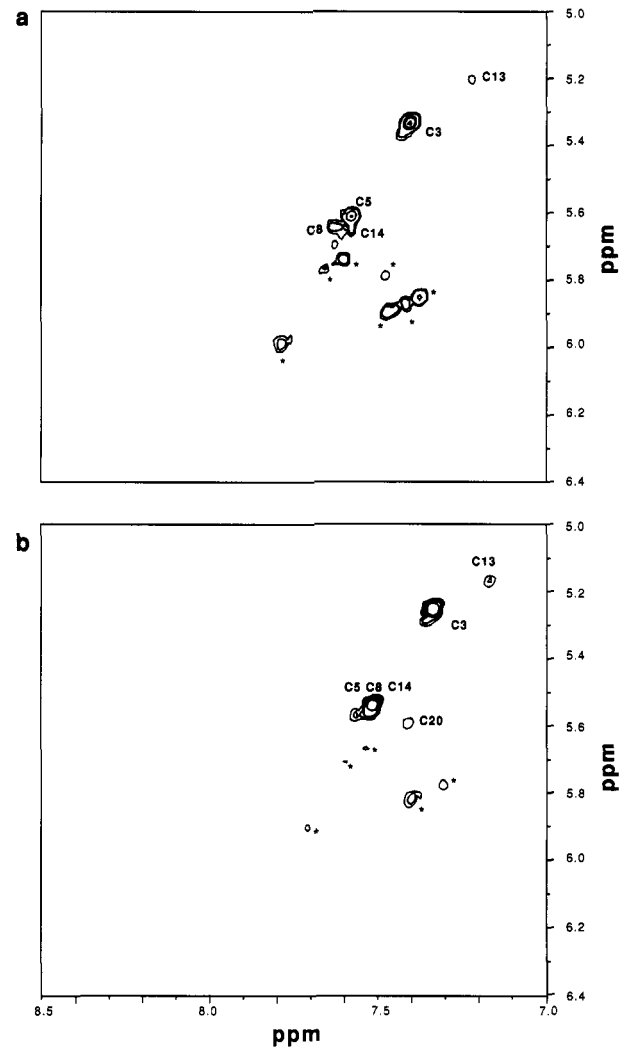

FIGURE 5: Expanded COSY contour plots of (a) the AF-modified (this study) and (b) the ABP-modified (Cho et al., 1992) 15-mer duplexes recorded in D_2O buffer at 27 °C. Cross peaks establish the scalar connectivities between the deoxycytidine H5 and H6 protons. Analogous interactions due to minor conformations are marked with asterisks.

with asterisks in Figure 2. These are assumed to be associated with NOE interactions displayed by imino protons of minor conformers. For instance, only one (7.53 ppm, peak 3) of the three moderately intense cross peaks found at 12.34 ppm in Figure 2b was positively assigned to the imino proton of [AF]-G11 in the major conformer. The two remaining cross peaks at 7.21 and 8.20 ppm (peaks *f and *g, respectively) appear to have stemmed from an overlapped deoxyguanosine imino proton of a minor conformer, whose presence could also be inferred from the anomalous melting behavior at 12.34 ppm (Figure 3, vide supra). Thus, although this signal started to melt at 32 °C, it subsisted in part at 40 °C, a temperature at which the same imino proton of the ABP-modified duplex had collapsed completely (Cho et al., 1992).

The observed change in the relative intensities of the G23 and G11 imino signals between 24 and 32 °C (Figure 3) provided additional support for the presence of more than one imino resonance at 12.34 ppm. Furthermore, two imino–imino proton interactions were detected at 12.34 ppm (peaks *h and *i, ~13.8 and 14.1 ppm, respectively, Figure 2c) that were not associated in any way with the [AF]G11 of the major conformer. These must be exchange cross peaks, which conceivably originated from a slow equilibrium with minor conformers. Moreover, there were additional strong NOE cross peaks of the presumed thymidine imino resonances at ~13.8 and 14.1 ppm (peaks *k, *l, and *m, Figure 2b), possibly reflecting NOE interactions with deoxyadenosine H2 protons; again, these cross peaks were not associated with the major conformer. However, the available NOE data were insufficient to allow any attempt at definite proton assignments of the cross peaks from the minor conformers.

Assignment of the Nonexchangeable Nucleic Acid Protons

Nonexchangeable Protons of the Major Conformer. An expanded portion of a 300-ms NOESY spectrum of the AF-modified duplex, recorded at 27 °C in D_2O buffer, is shown in duplicate in Figure 4. This contour plot outlines the sequential intrastrand NOE connectivities between the base H8/H6 protons (7.0–8.5 ppm) and the sugar H1′ and deoxycytidine H5 protons (5.0–6.5 ppm). The cross peaks

Table 2: Proton Chemical Shifts for the Major Conformer of the AF-Modified 15-mer Duplex in D_2O Buffer[a] and Chemical Shift Differences from the Corresponding Protons in the Unmodified 15-mer Duplex[b]

	H8/H6		H5/CH3		H1′		H2′		H2″		H3′	
base	AF 15-mer	Δδ[c]	AF 15-mer	Δδ	AF 15-mer	Δδ	AF 15-mer	Δδ	AF 15-mer	Δδ	AF 15-mer	Δδ
T1	7.27	+0.01	1.58	0.00	5.78	+0.01	1.61	−0.01	2.16	+0.02	4.62	0.00
A2	8.42	−0.01			6.29	0.00	2.87	−0.01	2.96	−0.03	5.03	−0.01
C3	7.41	−0.01	5.33	−0.01	5.90	0.00	2.07	−0.02	2.55	0.00	4.63	0.00
T4	7.44	0.00	1.54	0.00	5.61	+0.01	2.22	+0.04	2.52	+0.05	4.88	−0.01
C5	7.57	0.00	5.61	0.00	6.05	−0.01	NA[d]		NA		4.87	+0.01
T6	7.43	+0.01	1.62	0.00	6.03	−0.07	NA		NA		4.87	−0.01
T7	7.44	−0.02	1.64	0.00	5.64	−0.01	NA		NA		NA	
C8	7.59	+0.02	5.64	+0.01	6.06	**−0.11**	NA		NA		NA	
T9	NA		NA		NA		NA		NA		NA	
T10	NA		NA		NA		NA		NA		NA	
G11	NA				5.91	**−0.42**	NA		NA		NA	
A12	8.08	+0.07			6.18	+0.02	NA		2.84	+0.03	5.01	0.00
C13	7.23	+0.01	5.21	+0.03	5.96	**−0.15**	2.15	**−0.17**	2.52	**−0.14**	NA	
C14	7.57	0.00	5.65	0.00	6.14	−0.05	2.31	−0.05	2.50	−0.02	4.84	−0.02
T15	7.60	−0.03	1.79	−0.04	6.28	−0.02	2.31	−0.01	2.31	−0.01	4.58	−0.02
A16	8.06	−0.08			5.95	+0.01	2.37	+0.03	2.52	−0.01	NA	
G17	7.97	**−0.14**			NA		NA		NA		NA	
G18	NA				NA		NA		NA		NA	
T19	NA		*e*		NA		NA		NA		NA	
C20	NA		NA		NA		NA		NA		NA	
A21	NA				5.80	−0.05	NA		NA		NA	
A22	8.00	+0.01			6.10	**−0.26**	2.35	**+0.19**	2.60	**+0.16**	5.01	0.00
G23	7.56	−0.01			5.32	+0.01	2.43	−0.01	2.58	+0.01	4.94	0.00
A24	7.97	0.00			5.86	+0.01	2.53	0.00	2.79	+0.03	5.05	−0.04
A25	7.94	0.00			5.87	+0.01	2.54	−0.01	2.78	+0.01	5.02	−0.01
G26	7.52	0.00			5.44	+0.02	2.45	0.00	2.65	0.00	4.95	−0.01
A27	7.96	0.00			6.06	+0.01	2.62	−0.01	2.86	0.00	5.01	−0.07
G28	7.51	0.00			5.83	−0.01	2.37	0.00	2.59	0.00	4.89	0.00
T29	7.15	0.00	1.36	+0.01	5.94	0.00	1.92	+0.01	2.25	0.00	NA	
A30	8.28	0.00			6.37	−0.01	2.76	−0.01	2.53	0.00	4.71	−0.01

[a] Chemical shifts are reported in ppm downfield from TSP at 27 °C. Samples were dissolved in D_2O containing 100 mM NaCl, 10 mM sodium phosphate, and 100 μM disodium EDTA (pH 7.0) (D_2O buffer). The H4′ and H5′ protons were not assigned, except for the H5′-methylene protons of the 5′-terminal T1 (3.64 ppm) and A16 (3.68 ppm) nucleotides. [b] Taken from Cho et al. (1992). [c] Δδ = δ(unmodified 15-mer) − δ(AF-modified 15-mer); Δδ > 0.1 ppm are shown in boldface type. − indicates downfield shift and + indicates upfield shift of protons in the AF-modified 15-mer duplex. [d] Not assigned due to undetected or overlapped cross peaks. [e] Detected at 1.60 ppm in the NOESY spectrum taken in H_2O buffer (peak 43, Figure 2a).

between deoxycytidine H5 and H6 protons were readily recognized by their presence in the corresponding region of the COSY spectrum (Figure 5a) and are denoted by boldface characters in Figure 4 (i.e., **C3**, **C5**, **C8**, **C13**, and **C14**). Not unexpectedly (vide supra), the aromatic protons of C20 were not located. It should also be noted that the scalar H5/H6 COSY peak due to C13 was significantly weaker than those of the other deoxycytidines (Figure 5a). Similar anomalous behavior was encountered in the vicinity of the modification site (i.e., C13 and C20) for the ABP-modified duplex (Cho et al., 1992). Such effects have been attributed to decreased mobilities of the deoxycytidine residues (Borah et al., 1985). This may explain partially the difficulties experienced in locating the analogous scalar interaction due to C20 of the AF-modified duplex.

Most of the intrastrand sequential NOE connectivities between the base H8/H6 and the sugar H1′ protons of the AF-modified duplex could be traced using the general strategy applicable to typical B-DNA conformations (Hare et al., 1983; Feigon et al., 1983; Wüthrich, 1986). These sequential interactions in the noncoding and coding strands are linked by solid lines in Figure 4 (panels a and b, respectively). Such NOE connectivities could not be traced for the T9–T10–[AF]-G11 segment in the noncoding strand or for the G18–T19–C20 segment in the coding strand, since the corresponding cross peaks were either absent or too weak to be detected. The sugar H2′, H2″, and H3′ protons were assigned through a combined analysis of the NOESY and COSY spectra. However, since the interruptions in the sequential tracing mentioned above precluded the proper assignment of the H1′ protons in the T9–T10 and G17–G18–T19–C20 segments, the sugar H2′, H2″, and H3′ protons for these nucleotides could not be identified. In addition, extensive overlapping prevented the assignment of a majority of the H2′, H2″, and H3′ protons in the C5–T6–T7–C8 sequence. This also occurred with the ABP-modified duplex (Cho et al., 1992).

Several interbase cross peaks corresponding to interactions between the base H8/H6 protons and the H5 protons of 3′-flanking deoxycytidines (peaks a–c, Figure 4a) were observed for A2–C3, A12–C13, and C13–C14, respectively. Some additional weak NOE interactions involving deoxyadenosine H2 protons were also detected (peaks d–g, Figure 4a) and are assigned in the legend to Figure 4. It should be noted that the chemical shift values found in D_2O buffer for the deoxyadenosine H2 and the thymidine methyl protons differed slightly (~0.1 ppm) from those observed in H_2O buffer, presumably due to a combination of solvent and temperature effects. As with the unmodified and ABP-modified duplexes (Cho et al., 1992), the sugar H5′ protons in the 5′-terminal nucleotides (i.e., 3.64 and 3.68 ppm for T1 and A16, respectively) and the sugar H3′ protons in the 3′-terminal nucleotides (i.e., 4.58 and 4.71 ppm for T15 and A30, respectively) had characteristic upfield shifts relative to the corresponding protons in the other nucleotides.

The chemical shifts assigned to the majority of the nonexchangeable base and sugar protons of the AF-modified duplex are listed in Table 2, along with the measured chemical shift differences from their counterparts in the unmodified 15-mer duplex. The data in Table 2 illustrate that the conformational alteration elicited by the AF modification was

primarily limited to the nucleotides located in the vicinity of [AF]G11. This is evident from the fact that the chemical shift variations experienced upon adduct formation by the base and sugar protons of the nucleotides distant from the modification site were generally negligible (<0.1 ppm), indicating the adoption of a regular B-type double-helical DNA structure. Among the assigned sugar protons of the AF-modified duplex, fairly large deshieldings were observed for the H1′ protons of C13, [AF]G11, and A22, as well as for the H2′ and H2″ protons of C13; on the other hand, the H2′ and H2″ protons of A22 were shielded significantly (Table 2). All of these protons were located in nucleotides within two bases of the modification site. Of particular interest was the large deshielding (–0.42 ppm) of the H1′ proton of the AF-modified deoxyguanosine (Table 2), since the same proton exhibited a much less dramatic deshielding (–0.18 ppm) upon incorporation of ABP at G11 (Cho et al., 1992).

Several cross peaks of varying intensities that could not be assigned are marked with asterisks in Figure 4a. These cross peaks probably originated from minor conformers of the AF-modified duplex (vide infra); however, the possibility that some correspond to the unidentified intrastrand connectivities from the major conformer cannot be excluded. The absence of appropriate NOE cross peaks precluded any attempt to perform a detailed structural analysis of the AF modification site. Nonetheless, the available data indicated further that the AF adduct incorporated into the 15-mer duplex locally caused a more severe structural perturbation than that induced by its ABP analogue (Cho et al., 1992).

Nonexchangeable Protons of Minor Conformers. Figure 5a shows an expanded portion (7.0–8.5 vs 5.0–6.4 ppm) of the COSY spectrum of the AF-modified duplex, recorded in D_2O buffer at 27 °C. The only expected cross peaks in this region were the scalar coupling interactions between the H5 and H6 protons of individual deoxycytidines. The scalar cross peaks associated with the major conformer, which are labeled in Figure 5a, were identified through comparison with the NOESY spectrum recorded under identical conditions (Figure 4). Again, only the scalar interaction due to C20 remained undetected (vide supra).

In the same COSY spectrum, several additional intense cross peaks (marked with asterisks in Figure 5a) were observed that did not correspond to deoxycytidine H5/H6 scalar interactions of the major conformer. These extraneous cross peaks must have originated from identical scalar deoxycytidine interactions in minor conformers. Although adequate assignments could not be made, the cross-peak patterns were quite similar to those found for the minor conformer of the ABP-modified duplex (Cho et al., 1992) under the same experimental conditions (Figure 5b). This observation suggested that the two duplexes contained structurally similar minor conformers. Analysis of the COSY contour plots revealed that the scalar cross peaks associated with the minor conformers of the AF-modified duplex were substantially more intense than their counterparts in the ABP-modified duplex. From these data, the relative population of minor conformers of the AF-modified duplex was estimated to be greater than 40% at 27 °C, which is in agreement with the estimate from the 1D spectrum at 5 °C (Figure 1a, vide supra).

Assignment of the AF Protons. The 6.5–7.2-ppm region of the 1D proton spectrum of the AF-modified duplex recorded in D_2O buffer at 27 °C revealed several low-intensity proton signals at 6.68, 6.80, 6.87, 7.00, and 7.05 ppm (top of Figure 6a, arrows). Since nucleic acid protons do not typically resonate in this region, these signals were attributed to the

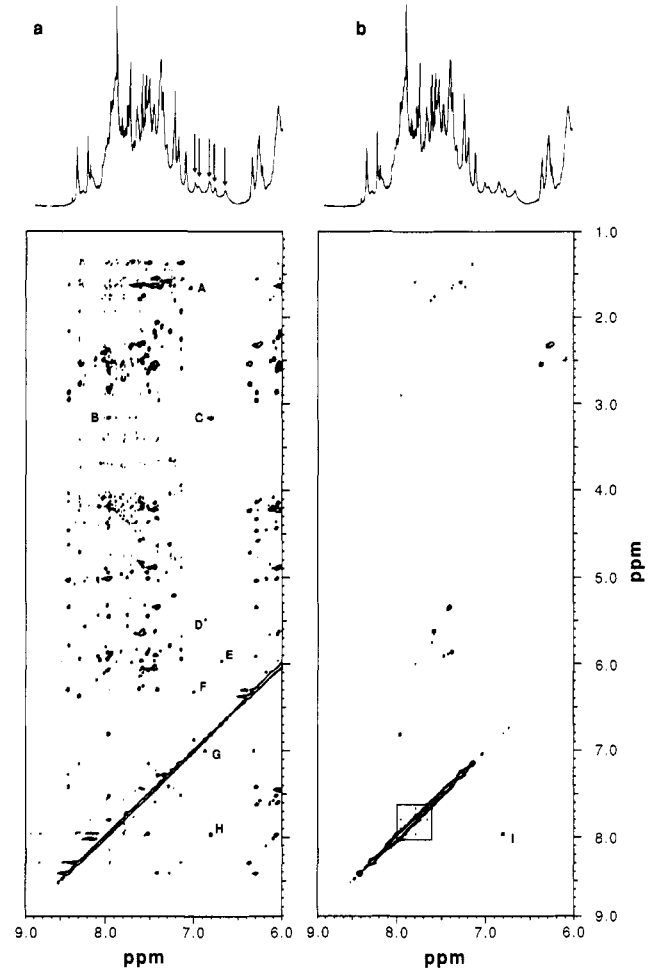

FIGURE 6: Expanded (a) 300-ms NOESY and (b) COSY contour plots of the AF-modified duplex in D_2O buffer at 27 °C, establishing NOE and scalar coupling connectivities, respectively, between the 6.0–9.0- and 1.0–9.0-ppm regions. The labeled cross peaks represent NOE (panel a) or scalar (panel b) connectivities between the AF aromatic protons and either nonexchangeable nucleic acid protons or other AF aromatic protons.

aromatic protons of AF. Despite the weak intensities of these resonances, integration of this region of the 1D spectrum appeared consistent with seven protons, assuming that the signal at 6.80 ppm represented one proton. Figure 6a shows an expanded portion (6.0–9.0 vs 1.0–9.0 ppm) of the 300-ms NOESY spectrum recorded in D_2O buffer at 27 °C. This region exhibits any possible NOE connectivities between the aromatic protons of AF and the nearby nucleic acid base and sugar protons. A small number of cross peaks (labeled with capital letters in Figure 6a) compatible with such interactions was observed.

A rather strong NOE cross peak (peak C, Figure 6a) was detected between the high-field aromatic resonance at 6.80 ppm and the AF geminal H9′,9″ protons at 3.15 ppm. This suggested that the aromatic resonance at 6.80 ppm could be assigned to one of the nearby protons of the AF moiety (i.e., H1 or H8). However, the remaining labeled cross peaks in Figure 6a could not be related unambiguously to specific base or sugar protons. The observed chemical shift range for the AF aromatic protons (6.7–7.1 ppm) represents substantial shielding as compared to the range (7.4–8.1 ppm) reported for the resonances of the AF aromatic protons of dG-C8-AF (Beland et al., 1980), which exists primarily in an anti conformation (Evans et al., 1980). This suggests that the AF fragment of the AF-modified duplex may be under the

influence of extensive stacking interactions, as would be expected with a syn alignment of the AF-modified deoxyguanosine. In fact, the observed chemical shift range (6.7–7.1 ppm) of the AF aromatic protons closely matched that (6.7–7.2 ppm) previously reported for the same protons of the AF-modified *syn*-deoxyguanosine in an 11-mer DNA duplex (Norman et al., 1989).

A second set of AF ring protons was detected further downfield, as indicated in the boxed region (7.6–8.0 ppm) of the COSY spectrum recorded in D_2O buffer at 27 °C (Figure 6b). The proton resonance at 7.95 ppm exhibited an NOE cross peak to the geminal H9′,9″ protons of AF at 3.15 ppm in the NOESY spectrum (peak B, Figure 6a), which suggested that it would be due to either the AF H1 or H8 proton. In addition, both the NOESY (peak H, Figure 6a) and the COSY (peak I, Figure 6b) spectra exhibited cross peaks reflecting an interaction between the 7.95-ppm proton in the second set of AF resonances and the 6.80-ppm proton in the first set of resonances (vide supra). This may be due to a saturation transfer between the same AF protons (i.e., H1 or H8, which flanked the geminal H9′,9″ protons) of two slowly interchanging conformers. Even though the specific assignments of the AF resonances at 7.6–8.0 ppm were not made, this chemical shift range closely matched that (7.4–8.1 ppm) reported for dG-C8-AF (Beland et al., 1980). The finding of a second set of AF protons not only supported the existence of multiple conformations but also explained the low intensities observed for the upfield AF protons (vide supra).

Despite the uncertainty about the exact conformational alignment at the modification site, the data discussed in the previous sections suggested that the AF resonances at 7.6–8.0 ppm were associated with the major conformer of the AF-modified duplex. This conformer appeared to be a relatively unperturbed B-type double-helical structure, with an essentially unstacked AF moiety rapidly rotating in the major groove, as was established for the major conformer of the ABP-modified duplex. On the other hand, the AF resonances at 6.7–7.1 ppm were collectively shielded as a result of possible stacking or van der Waals interactions and seemed to be associated with the minor conformers of the AF-modified duplex.

DISCUSSION

Multiple Conformations. The present NMR study has focused on the conformational consequences induced by the incorporation of a single dG-C8-AF adduct in a 15-mer DNA duplex sequence, spanning a portion of the mouse c-Ha-*ras* protooncogene centered around codon 61.

We found clear evidence that, on the NMR time scale, the AF-modified duplex adopts multiple slow-exchanging conformations in solution, with one being major (~60%). This conclusion was based on the following observations: (1) the downfield region of the 1D proton spectrum in H_2O buffer (Figure 1a) exhibited more than 15 imino proton resonances of different intensities; (2) medium to strong cross peaks unrelated to the major conformer were detected in the NOESY spectra recorded in H_2O (Figure 2, panels b and c) and D_2O buffers (Figure 4); (3) the COSY spectrum (Figure 5a) displayed several medium to strong deoxycytidine H5–H6 coupling interactions that were not associated with the major conformer; and (4) at least two sets of aromatic AF protons were present in the NOESY and COSY spectra recorded in D_2O buffer (Figure 6, panels a and b, respectively), and some of these protons appeared to be involved in saturation transfer.

Conformational heterogeneities are induced by multiple-conformer equilibria and appear to be commonly associated with arylamine-modified DNA duplexes. For example, Patel and co-workers were unable to conduct a detailed NMR study on an AF-modified 11-mer DNA duplex containing a G:C base pair at the modification site, since the ^1H NMR spectrum of the duplex displayed a mixture of narrow and broad lines (Norman et al., 1989). They were successful, however, in characterizing the same 11-mer DNA duplex containing a {syn}[AF]G:{anti}A base pair, which exhibited exclusively one conformation. Similar conformational heterogeneity was noted in the proton NMR study of a 9-mer DNA duplex modified by AAF (O'Handley et al., 1993), for which the population of the major conformer was about 70%. We have also shown (Cho et al., 1992) that an ABP-modified 15-mer DNA duplex analogous to the AF-modified duplex studied in the current experiment exists in solution as an equilibrium mixture of at least two slowly exchanging conformations, with one being predominant (>90%). Not unexpectedly, our initial attempts to perform a detailed NMR analysis of the AF-modified duplex were hampered by the conformational heterogeneity discussed above. However, the assignment process was greatly aided by the availability of spectral information on the parent unmodified and ABP-modified duplexes, which have been characterized relatively well (Cho et al., 1992). The simplification was due in part to the fact that the AF-modified duplex adopted major and minor conformations essentially similar to those of the ABP-modified duplex, although the conformer ratios clearly were different (vide infra).

Major Conformer of the AF-Modified Duplex. We obtained sufficient evidence that the structure of the major conformer of the AF-modified duplex was essentially identical to that of the major conformer adopted by its ABP-modified analogue, i.e., a relatively unperturbed B-type double helix, with the arylamine moiety rotating in the major groove. Thus, (1) a major portion of the 1D imino spectral pattern of the AF-modified duplex (Figure 1a) closely resembled that of the ABP-modified duplex (Figure 1b); (2) the NOESY spectra of the AF-modified duplex, both in H_2O (e.g., Figure 2) and D_2O buffers (e.g., Figure 4), revealed a major conformer displaying NOE interactions strikingly similar to those previously observed for the major conformer of the ABP-modified duplex; and (3) the major portions of the 1D imino proton region exhibited similar temperature-dependent sequential broadenings for the two duplexes.

The overall structural information on the major conformer could be deduced from a comparison of the spectral pattern of the exchangeable protons with that of the corresponding region of the unmodified duplex. We have previously shown (Cho et al., 1992) that the unmodified duplex adopts a standard Watson–Crick B-type DNA conformation throughout its entire length, with the possible exception of the frayed oligonucleotide ends. As shown in Table 1, the chemical shift changes that occurred for the exchangeable imino protons as a consequence of adduct formation were almost negligible at 5 °C (<0.06 ppm). The exceptions were those at ([AF]G11) or adjacent to (T10 and T19) the modification site, with the most significant effect on T10.

The deoxyadenosine H2 protons, as well as the hydrogen-bonded and exposed deoxycytidine amino protons of base pairs distant from the AF modification site, were also essentially unaffected upon adduct formation. Importantly, the chemical shift variations observed for most of the nonexchangeable deoxyadenosine H2 protons and the exchangeable protons of the AF-modified duplex (Table 1) were comparable to those found for the same protons of the ABP-modified duplex; in

this regard, substantial shielding of the T10 imino proton with both compounds was particularly significant. This observation implies that the major conformers of the two duplexes shared the same structural features, including those in the vicinity of the adduct site. Nonetheless, the imino proton of T19 and the deoxyadenosine H2 proton of A12 in the A12:T19 base pair flanking the AF-modified G11 in the 3′-direction were shielded upon adduct incorporation (Table 1), while the opposite effect was observed with the ABP-modified duplex. Furthermore, some NOE cross-peak patterns associated with base pairs at or near the AF modification site were not clearly defined (Figure 2). Notable examples were the expected NOEs from interactions between the imino proton of G11 and the H5 or each of the amino protons of C20, as well as between the same imino proton and the imino protons of T10 and T19 in the flanking A21:T10 and A12:T19 base pairs. It should be noted that all the cross peaks arising from these interactions were detected for the ABP-modified duplex (Cho et al., 1992). In addition, a unique deshielding (−0.3 and −0.4 ppm) observed for the T19 methyl protons (peak 43, Figure 2a), as compared to those of the unmodified and ABP-modified duplex, respectively (Cho et al., 1992), indicated an alteration in the stacking with nearby bases. Taken together, these observations strongly indicate that the conformational perturbation at the adduct site was more severe for the major conformer of the AF-modified duplex than for the major conformer of its ABP-modified analogue.

The NOE connectivities observed between the base H8/H6 and the sugar H1′ protons in D_2O buffer (Figure 4) indicated the formation of an overall right-handed helix. However, some proton assignments, in particular those regarding base and sugar protons at and near the modification site, were difficult (Table 2) due to the absence of the cross peaks needed to establish the sequential connectivities. This is further evidence that the local perturbation induced by dG-C8-AF in the 15-mer duplex was more significant than that caused by dG-C8-ABP in the same duplex.

The absence of most of the NOE connectivities associated with the imino, base, and sugar protons corresponding to the T9–T10–[AF]G11–A12 and A21–C20–T19–G18 segments prevented us from defining the conformation of the modified deoxyguanosine. However, we found a set of aromatic AF resonances in a chemical shift range (7.6–8.0 ppm) comparable to that reported for dG-C8-AF (Beland et al., 1980). Although the proper assignment of these resonances could not be made, the chemical shift range exhibited by these AF protons was consistent with the absence of significant stacking interactions between the fluorene moiety and the helix. This may explain the absence of NOE interactions between this set of AF resonances and protons in the neighboring nucleotides.

Minor Conformers of the AF-Modified Duplex. As addressed above, the evidence for the existence of minor conformers of the AF-modified duplex was overwhelming. The estimated extent (30–40%) of these conformers is much greater than that (5–10%) previously found for the ABP-modified duplex (Cho et al., 1992). Although insufficient data prevented a detailed characterization of the minor conformers of the AF-modified duplex, a comparative NMR analysis suggested that the conformational characteristics should be similar to those of the minor conformer adopted by the ABP-modified duplex. This conclusion was based on two crucial factors. First, a set of aromatic AF protons resonated at 6.7–7.1 ppm, a range that closely resembles that (6.5–6.9 ppm) encountered for the ABP protons belonging to the minor conformer of the ABP-modified duplex. Second, the pattern of cross peaks observed in the COSY spectrum for deoxycytidine H5–H6 scalar interactions associated with minor conformers (Figure 5a) was remarkably similar to that corresponding to identical interactions associated with the minor conformer of the ABP-modified duplex (Figure 5b).

Since the detailed structural characterization of the minor conformers of the ABP-modified duplex has not been achieved (Cho et al., 1992), we could not use that information as a starting point to further probe the minor conformations of the AF-modified duplex. However, the AF protons for the minor conformer were collectively shielded in comparison to those normally found in dG-C8-AF (vide supra). The chemical shift range (6.7–7.1 ppm) observed for the minor AF-modified conformer closely matched those reported for AF- (6.7–7.2 ppm) and AAF-modified (6.4–7.3 ppm) *syn*-deoxyguanosines in DNA duplexes [Norman et al. (1989) and O'Handley et al. (1993), respectively], in which the arylamine moieties experienced extensive stacking and/or van der Waals interactions. It should also be noted that the deoxycytidine aromatic protons of the minor conformers were collectively shielded in both the AF- and ABP-modified duplexes compared to those of the corresponding major conformer, further substantiating the above argument. Structural possibilities for the minor conformer include a syn AF-modified G11 with insertion of the fluorene moiety into the helix or, alternatively, a Hoogsteen-type base pairing at the modification site, both of which are consistent with extensive stacking of the arylamine in the minor groove of the helix. Several other alignment models that may be relevant to these structural features have been proposed (Shapiro et al., 1989; Broyde et al., 1990).

Biological Implications of the Conformational Heterogeneity. The partial characterization of minor conformers of the ABP- (Cho et al., 1992) and AF-modified duplexes (this study) is significant, since the extensive stacking of the arylamine fragment found in these conformations represents a dramatic structural perturbation that may provide a rationale for arylamine mutagenesis. Furthermore, the differences in the conformer ratios of essentially identical major and minor contributors exhibited by the two modified duplexes may also be important for the distinct biological responses associated with the arylamines involved. The low contribution (<10%) of the minor conformers of the ABP-modified duplex, compared to that (30–40%) estimated for its AF-modified analogue, must reflect a direct consequence of structural differences in the arylamine moieties. Thus, the higher conformer heterogeneity found for the AF-modified duplex is probably related to a higher overlapping efficiency of the planar AF aromatic ring than of the twisted ABP ring with the nearby bases. In this regard, it is worth recalling that, compared to dG-C8-AF, dG-C8-ABP exhibits lower frameshift mutagenesis in *S. typhimurium* TA1538, is more resistant to DNA repair enzymes in the livers of dogs (Beland & Kadlubar, 1990), and is a weaker hepatocarcinogen in mice (Beland et al., 1992). Also consistent with this argument are recent findings on the mutagenic potentials of several arylamine C8-deoxyguanosine adducts incorporated in pBR322, in which planar arylamines (e.g., AF and 1-aminopyrene) showed higher mutagenicity than nonplanar arylamines (e.g., ABP and *N*-acetylbenzidine) (W. B. Melchior, M. M. Marques, and F. A. Beland, submitted for publication).

REFERENCES

Aue, W. P., Bartholdi, E., & Ernst, R. R. (1976) *J. Chem. Phys. 64*, 2229–2246.

Basu, A. K., & Essigmann, J. M. (1988) *Chem. Res. Toxicol. 1*, 1–18.

Beland, F. A., & Kadlubar, F. F. (1990) in *Handbook of Experimental Pharmacology* (Cooper, C. S., & Grover, P. L., Eds.) Vol. 94/I, pp 267–325, Springer-Verlag, Heidelberg, Germany.

Beland, F. A., Allaben, W. T., & Evans, F. E. (1980) *Cancer Res. 40*, 834–840.

Beland, F. A., Fullerton, N. F., Smith, B. A., & Poirier, M. C. (1992) in *Relevance of Animal Studies to the Evaluation of Human Cancer Risk* (D'Amato, R., Slaga, T. J., Farland, W. H., & Henry, C., Eds.) pp 79–92, Wiley-Liss, New York.

Bodenhausen, G., Kogler, H., & Ernst, R. R. (1984) *J. Magn. Reson. 58*, 370–388.

Boelens, R., Scheek, R. M., Dijkstra, K., & Kaptein, R. (1985) *J. Magn. Reson. 62*, 378–386.

Borah, B., Roy, S., Zon, G., & Cohen, J. S. (1985) *Biochem. Biophys. Res. Commun. 133*, 380–388.

Broyde, S., & Hingerty, B. (1983) *Biopolymers 22*, 2423–2441.

Broyde, S., Hingerty, B. E., & Srinivasan, A. R. (1985) *Carcinogenesis 6*, 719–725.

Broyde, S., Hingerty, B. E., Shapiro, R., & Norman, D. (1990) in *Nitroarenes: Occurrence, Metabolism, and Biological Impact* (Howard, P. C., Hecht, S. S., & Beland, F. A., Eds.) pp 113–123, Plenum Press, New York.

Cho, B. P., Beland, F. A., & Marques, M. M. (1992) *Biochemistry 31*, 9587–9602.

Evans, F. E., & Miller, D. W. (1982) *Biochem. Biophys. Res. Commun. 108*, 933–939.

Evans, F. E., & Levine, R. A. (1987) *Biopolymers 26*, 1035–1046.

Evans, F. E., & Levine, R. A. (1988) *Biochemistry 27*, 3046–3055.

Evans, F. E., Miller, D. W., & Beland, F. A. (1980) *Carcinogenesis 1*, 955–959.

Evans, F. E., Miller, D. W., & Levine, R. A. (1984) *J. Am. Chem. Soc. 106*, 396–401.

Feigon, J., Leupin, W., Denny, W. A., & Kearns, D. R. (1983) *Biochemistry 22*, 5943–5951.

Hare, D. R., Wemmer, D. E., Chou, S.-H., Drobny, G., & Reid, B. R. (1983) *J. Mol. Biol. 171*, 319–336.

Harris, T. M., Stone, M. P., & Harris, C. M. (1988) *Chem. Res. Toxicol. 1*, 79–96.

Hingerty, B. E., & Broyde, S. (1986) *J. Biomol. Struct. Dyn. 4*, 365–372.

Hore, P. J. (1983) *J. Magn. Reson. 55*, 283–300.

Kadlubar, F. F., Beland, F. A., Beranek, D. T., Dooley, K. L., Heflich, R. H., & Evans, F. E. (1982) in *Environmental Mutagens and Carcinogens* (Sugimura, T., Kondo, S., & Takebe, H., Eds.) pp 385–396, Liss, New York.

Lasko, D. D., Basu, A. K., Kadlubar, F. F., Evans, F. E., Lay, J. O., Jr., & Essigmann, J. M. (1987) *Biochemistry 26*, 3072–3081.

Leng, M., Ptak, M., & Rio, P. (1980) *Biochem. Biophys. Res. Commun. 96*, 1095–1102.

Lipkowitz, K. B., Chevalier, T., Widdifield, M., & Beland, F. A. (1982) *Chem.-Biol. Interact. 40*, 57–76.

Marques, M. M., & Beland, F. A. (1990) *Chem. Res. Toxicol. 3*, 559–565.

Neidle, S., Kuroda, R., Broyde, S., Hingerty, B. E., Levine, R. A., Miller, D. W., & Evans, F. E. (1984) *Nucleic Acids Res. 12*, 8219–8233.

Norman, D., Abuaf, P., Hingerty, B. E., Live, D., Grunberger, D., Broyde, S., & Patel, D. J. (1989) *Biochemistry 28*, 7462–7476.

O'Handley, S. F., Sanford, D. G., Xu, R., Lester, C. C., Hingerty, B. E., Broyde, S., & Krugh, T. R. (1993) *Biochemistry 32*, 2481–2497.

Sage, E., & Leng, M. (1980) *Proc. Natl. Acad. Sci. U.S.A. 77*, 4597–4601.

Shapiro, R., Underwood, G. R., Zawadzka, H., Broyde, S., & Hingerty, B. E. (1986) *Biochemistry 25*, 2198–2205.

Shapiro, R., Hingerty, B. E., & Broyde, S. (1989) *J. Biomol. Struct. Dyn. 7*, 493–513.

Sharma, M., & Box, H. C. (1985) *Chem.-Biol. Interact. 56*, 73–88.

Van Geet, A. L. (1968) *Anal. Chem. 40*, 2227–2229.

van Houte, L. P. A., Bokma, J. T., Lutgerink, J. T., Westra, J. G., Retèl, J., van Grondelle, R., & Blok, J. (1987) *Carcinogenesis 8*, 759–766.

van Houte, L. P. A., Westra, J. G., Retèl, J., & van Grondelle, R. (1988) *Carcinogenesis 9*, 1017–1027.

Wemmer, D. E. (1992) in *Biological Magnetic Resonance: Carbohydrates and Nucleic Acids* (Berliner, L. J., & Reuben, J., Eds.) pp 195–264, Plenum Press, New York.

Wiseman, R. W., Stowers, S. J., Miller, E. C., Anderson, M. W., & Miller, J. A. (1986) *Proc. Natl. Acad. Sci. U.S.A. 83*, 5825–5829.

Wüthrich, K. (1986) *NMR of Proteins and Nucleic Acids*, Wiley-Interscience, New York.